Thermochimica Acta, 125 (1988) 99-106
Elsevier Science Publishers B.V., Amsterdam - Printed in The Netherlands

KINETIC MODEL FOR THE CARBOTHERMIC REDUCTION OF MANGANESE DIOXIDE

M.A. REUTER and J.S.J. VAN DEVENTER

Department of Metallurgical Engineering, University of Stellenbosch, Stellenbosch 7600 (South Africa)

(Received 26 May 1987)

ABSTRACT

Mixtures of MnO_2 and graphite were reacted under argon at different constant temperatures, and the loss in mass was recorded continuously. The reduction path was assumed to be $MnO_2 \rightarrow Mn_3O_4 \rightarrow MnO \rightarrow Mn_5C_2$ or Mn. Chemical conditions determine the ratio of Mn_5C_2/Mn formed in the reduction product. A multi-step shrinking-core model was proposed to describe the kinetics of reduction. Parameters in this model were estimated by performing a least-squares regression on the experimental data. Acceptable correspondence was obtained between predicted and experimental kinetic curves. The activation energy for the reduction of MnO_2 to Mn_3O_4 was only 71.3 kJ mol^{-1}, which indicated a weak dependence on temperature. Further reduction steps revealed activation energies of about 207 kJ mol^{-1}, and were of the same order of magnitude as the activation energy for the Boudouard reaction. The distribution of species at any point in time, which depended on the MnO_2/carbon ratio and the temperature, could be calculated by means of this proposed model.

LIST OF SYMBOLS

A_j	Constant in the Arrhenius equation(s)
α	Fraction of reduced MnO which forms Mn_5C_2
e	Defined by eqn. (8)
E_j	Activation energy for reaction j (kJ mol^{-1})
f	Defined by eqn. (9)
j	Indicating reaction (1), (2), (3) or (4)
m_1	Molecular mass of MnO_2 (g mol^{-1})
m_2	Molecular mass of C (g mol^{-1})
n	Number of data points
R	Universal gas constant (kJ mol^{-1} K^{-1})
S	Standard error in regression
t	Time (s)

0040-6031/88/$03.50

τ_j	Time required for the completion of reaction j (s)
T	Absolute temperature (K)
X	Total conversion of MnO_2, as defined by eqns. (11) and (12)
X_{exp}	Total conversion of MnO_2 measured experimentally
X_j	Conversion for reaction j, as defined by eqn. (5)
x	Mass of MnO_2 (g)
y	Mass of C (g)

INTRODUCTION

Manganese is an important alloying element in the formation of ferroalloys. The manganese is added to steel mostly as a ferroalloy, produced in submerged-arc furnaces by the reduction of manganese ore by carbon.

A number of models has been proposed to explain the path of reduction of manganese oxides and ore to either manganese metal or manganese carbide. Grimsley et al. [1] established that the reduction path is $MnO_2 \rightarrow Mn_3O_4 \rightarrow MnO \rightarrow Mn_7C_3$, and proposed a kinetic model for the reduction of Mn_3O_4 to Mn_7C_3. The reaction rate was taken to be a function of the CO concentration.

Koursaris and See [2] found that manganosite (MnO) is reduced to the carbide and Mn metal, either by the reduction of manganosite by solid carbon or by the reduction by carbon saturated alloy. Rankin and van Deventer [3] observed that Mn_5C_2 is the carbide that forms during the reduction of manganosite by graphite. They found that the activation energy of reduction was 241 kJ mol^{-1}. This was very similar to the activation energy of 257 kJ mol^{-1} measured for the gasification of graphite by CO_2. According to van Deventer [4] the presence of gangue components may influence the metal/carbide ratio in the reduction product.

De Bruijn et al. [5] fitted a shrinking-core model and a crackling-core model to the two-stage reduction of MnO_2 to MnO by H_2 which proceeded via Mn_3O_4. The crackling-core model fitted the data well, although no provision was made for equilibrium conversions lower than unity.

King and Brown [6] developed a two-stage kinetic model for the reduction of Mn_3O_4 by carbon. The reaction rate was considered to be a function of the diffusion rate of CO. The proposed reaction path was $Mn_3O_4 \rightarrow MnO \rightarrow Mn_7C_3$. Equilibrium conversions lower than unity were not considered.

In this paper a four-step shrinking-core reduction model is proposed in which all reaction fronts shrink simultaneously. The last two steps run in parallel. The suggested reaction path is $MnO_2 \rightarrow Mn_3O_4 \rightarrow MnO \rightarrow Mn_5C_2$ or Mn, where Mn_5C_2 and Mn form simultaneously. Contrary to previously published models for the reduction of manganese oxides, equilibrium conversions lower than unity are taken into account.

KINETIC MODEL

Assumptions and definitions

The following six points form the basis for the formulation of the model:

(a) Only CO is present, i.e. the temperature is sufficiently high in order to shift the Boudouard reaction ($C + CO_2 \rightarrow 2CO$) almost completely to the right.

(b) The following four reactions proceed simultaneously at different rates

$$3MnO_2 + 2C = Mn_3O_4 + 2CO \tag{1}$$

$$Mn_3O_4 + C = 3MnO + CO \tag{2}$$

$$5MnO + 7C = Mn_5C_2 + 5CO \tag{3}$$

$$MnO + C = Mn + CO \tag{4}$$

Reactions (1) and (2) go to completion, while reactions (3) and (4) run in parallel. A fraction of the MnO formed follows reaction (3) and a fraction follows reaction (4). These fractions are functions of the chemical conditions and could be dependent on the nature of impurities present [4]. It does not seem to be possible to extrapolate the fractions of MnO following reactions (3) and (4) from one system to another.

(c) Chemical reaction is rate controlling, in other words the following model [7] defines the conversion of each of the four simultaneous shrinking cores as depicted in Fig. 1

$$X_j = 1 - \left(1 - t/\tau_j\right)^3 \qquad \text{for } j = 1, 2, 3, 4 \tag{5}$$

where 1, 2, 3 and 4 refer to reactions (1)–(4). Each reaction has its own rate of reaction and therefore its own τ_j, which is dependent on temperature according to the Arrhenius relationship

$$\tau_j = A_j \exp\left(E_j/RT\right) \tag{6}$$

Figure 1 shows the regions that may exist in an MnO_2 particle at time t before reaction (1) is completed. At this point in time, four regions exist in the particle, viz. a core of MnO_2, internal shells of Mn_3O_4 and MnO, and an external layer consisting of both Mn and Mn_5C_2. A shrinking-core mechanism during the reduction of manganese oxides was also observed by Grimsley et al. [1] and De Bruijn et al. [5].

(d) The total conversion X is defined as the ratio of the oxygen removed from the MnO_2 to the total amount of oxygen removable initially.

(e) Assume that x gram of MnO_2 (x/m_1 moles) and y gram of C (y/m_2 moles) are used. Hence, the amount of O to be removed from MnO_2 is $2(x/m_1)$ moles.

(f) Of the MnO which is actually reduced, a fraction α forms Mn_5C_2 and a fraction $(1 - \alpha)$ forms Mn at equilibrium.

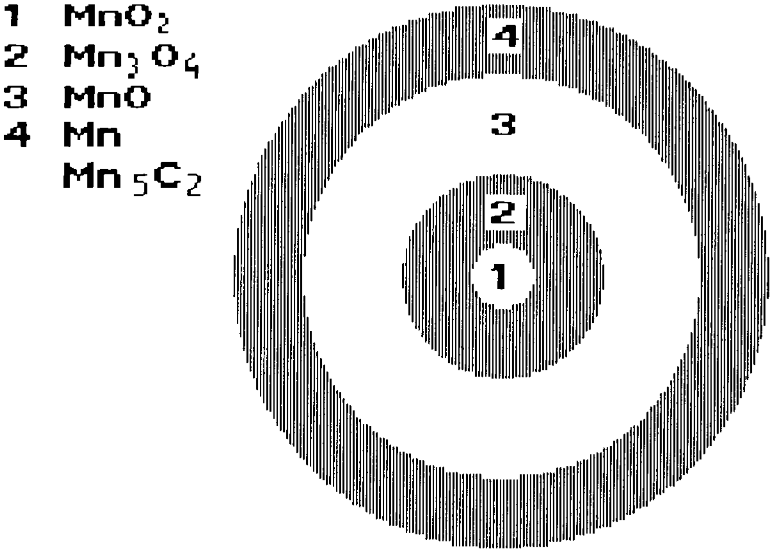

Fig. 1. The four simultaneous shrinking cores.

(g) If it is assumed that no MnO or C remains in the reaction product at equilibrium, it can be shown that

$$(y/m_2) = 2(x/m_1)(1-\alpha) + (12/5)(x/m_1)\alpha \tag{7}$$

This equation determines whether an excess of carbon is partaking in the reduction [i.e. left hand side is larger than the right hand side in eqn. (7)]. If an excess of carbon is used it is assumed that no MnO is left in the reduction product.

Model formulation

From stoichiometric considerations, the following may be stated:

(a) The total amount of oxygen liberated by reaction (1) is $(2/3)(x/m_1)$ moles.

(b) If reaction (1) goes to completion, the total amount of oxygen liberated by reaction (2) is $(1/3)(x/m_1)$ moles.

(c) If reaction (2) goes to completion in the presence of a deficiency of carbon, it can be shown that reaction (3) liberates e moles of oxygen and reaction (4) liberates f moles of oxygen, where

$$e = \frac{5\alpha(y/m_2 - x/m_1)}{(2\alpha + 5)} \tag{8}$$

$$f = \frac{5(1-\alpha)(y/m_2 - x/m_1)}{(2\alpha + 5)} \tag{9}$$

(d) Under the conditions stated in (c), the total molar quantity of oxygen liberated at time t is given by the following expression

$$O_{(\text{liberated})} = (x/m_1)\left[(2/3)X_1 + (1/3)X_2 + eX_3 + fX_4\right] \tag{10}$$

(e) The total conversion X may hence be formulated by dividing eqn. (10) by $2(x/m_1)$

$$X = (1/3)X_1 + (1/6)X_2 + (m_1/2x)eX_3 + (m_1/2x)fX_4 \tag{11}$$

(f) In the event of eqn. (7) predicting an excess amount of carbon partaking in the reduction, eqn. (10) reduces to

$$X = (1/3)X_1 + (1/6)X_2 + (1/2)\alpha X_3 + (1/2)(1-\alpha)X_4 \tag{12}$$

Model parameters

Equations (5), (6), (8), (9) and either eqn. (11) or (12) subject to (7) should be used simultaneously in order to calculate kinetic curves. The parameters A_j, E_j and α could be estimated by performing a least-squares regression on the experimental kinetic data. The search routine used in the multi-variable regression program converged when the standard error S was minimized

$$S = \left(\frac{\sum (X - X_{\text{exp}})^2}{n-1}\right)^{1/2} \tag{13}$$

EXPERIMENTAL

The experimental techniques used were similar to those described in earlier papers [3,4]. Analytical grade MnO_2 (2.0 g) and various quantities of high-purity graphite were used. The reduction experiments were conducted

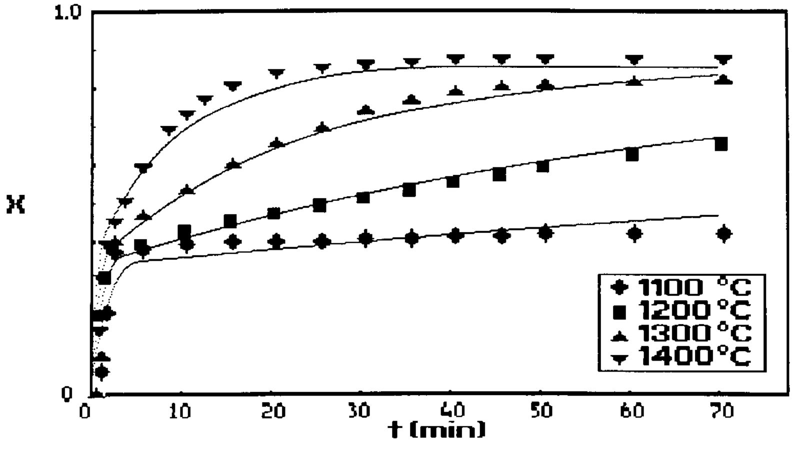

Fig. 2. Kinetic model (solid line) fitted to reduction data at different constant temperatures and equimolar quantities of MnO_2 and C.

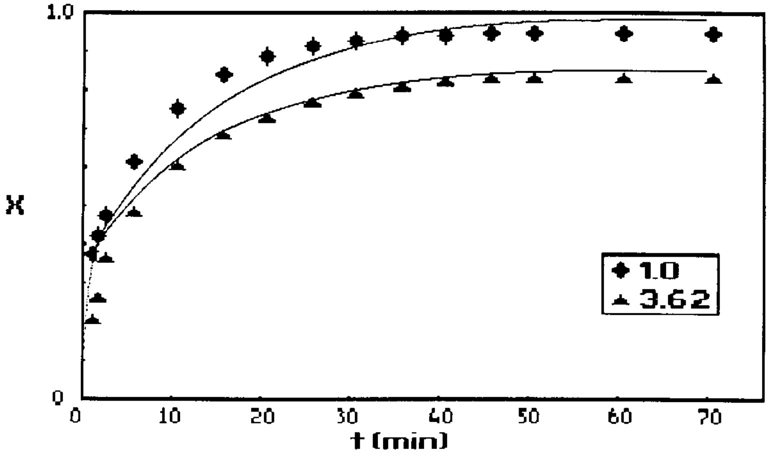

Fig. 3. Kinetic model (solid line) fitted to reduction data at a constant temperature of 1350 ° C and two different mass ratios of MnO_2 to C.

under argon in a vertical tube furnace fitted with a continuous weighing and recording electronic balance.

In the first set of experiments equimolar quantities of MnO_2 and graphite were mixed intimately at constant temperatures of 1100, 1200, 1300 and 1400 ° C. Results are given in Fig. 2.

The second set of experiments involved the reduction of dissimilar molar quantities of MnO_2 and graphite at a constant temperature of 1350 ° C. The mass ratios of MnO_2 to graphite used were 3.62 (equimolar) and 1.0. Figure 3 shows the experimental reduction curves.

RESULTS AND DISCUSSION

Figure 2 shows the experimental data as well as the curves predicted by the theoretical model for the reduction of equimolar quantities of MnO_2 and graphite at different constant temperatures. The standard error S between the model predictions and the experimental data lies between 0.02 and 0.04 for the temperature range 1100–1400 ° C. Acceptable correspondence was obtained between experimental data and model predictions. The parameters A_j, E_j and α were estimated simultaneously during a regression analysis on the data. The model parameters could be correlated by the following Arrhenius equations for $\alpha = 0.96$, with correlation coefficient between 0.99 and 1.0

$$\tau_1 = 1.16 \times 10^{-2} \exp(8575/T) \tag{14}$$

$$\tau_2 = 3.36 \times 10^{-6} \exp(25618/T) \tag{15}$$

$$\tau_3 = 1.56 \times 10^{-5} \exp(24736/T) \tag{16}$$

$$\tau_4 = 4.23 \times 10^{-4} \exp(24841/T) \tag{17}$$

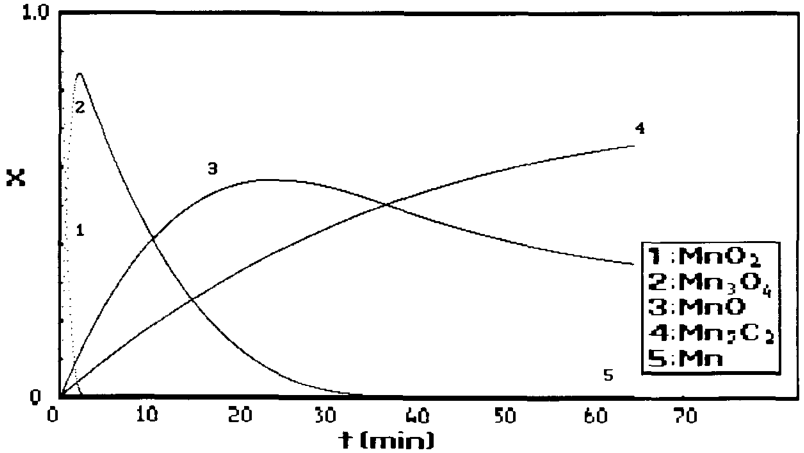

Fig. 4. Formation and disappearance of Mn species at 1300 ° C and equimolar quantities of MnO_2 and C.

The first reaction step, i.e. the reduction of MnO_2 to Mn_3O_4, exhibits an activation energy of only (8575 × 8.314) or 71.3 kJ mol^{-1} which supports the experimental observation of a weak temperature dependence. However, the activation energies for the other three reactions are 213, 206 and 207 kJ mol^{-1} respectively and lie in the same region as the 257 kJ mol^{-1} reported for the Boudouard reaction [3]. This provides some evidence that the Boudouard reaction plays a role in the reduction, especially in the last three reactions.

Figure 3 depicts the data obtained in reduction experiments at a constant temperature of 1350 ° C and mass ratios *x*/*y* of 3.62 and 1.0 respectively. An

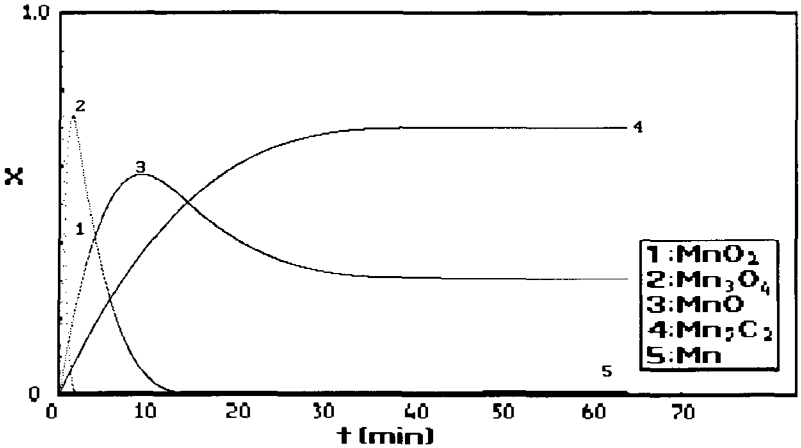

Fig. 5. Formation and disappearance of Mn species at 1400 ° C and equimolar quantities of MnO_2 and C.

increase in the carbon content appears to increase the conversion and the formation of carbide [3]. The other model parameters are given by eqns. (14)–(17) for $\alpha = 0.96$. The theoretical model fits the experimental data reasonably well for the case where $x/y = 3.62$. However, for the case where $x/y = 1.0$ it appears as if the kinetics were faster than predicted by the model.

Figures 4 and 5 depict the formation and disappearance of the various Mn-species, as predicted by the theoretical model, for different constant temperatures and a mass ratio of MnO_2 to graphite of 3.62. Curve 1 shows the disappearance of MnO_2, curve 2 the formation and subsequent disappearance of Mn_3O_4, curve 3 the formation and disappearance of MnO, curve 4 the formation of Mn_5C_2, and curve 5 the formation of Mn.

CONCLUSIONS

The proposed kinetic model fits the experimental reduction data reasonably well. This provides some evidence that the multi-step shrinking-core mechanism is representative of the real process. Different levels of equilibrium conversion could be modelled satisfactorily. The kinetics of reduction of MnO_2 to Mn_3O_4 showed a weak dependence on temperature and an activation energy of only 71.3 kJ mol^{-1}. Further reduction of Mn_3O_4 to MnO, MnO to Mn, and MnO to Mn_5C_2 revealed activation energies of 213, 206 and 207 kJ mol^{-1}, which were in the same region as the activation energy for the Boudouard reaction. When the graphite/MnO_2 ratio increases the model predicts correctly an increase in the conversion.

REFERENCES

1 W.D. Grimsley, J.B. See and R.P. King, J. S. Afr. Inst. Min. Metall., 77 (1977) 51.
2 A. Koursaris and J.B. See, Report no. 1975, National Institute for Metallurgy, Johannesburg, 1978.
3 W.J. Rankin and J.S.J. van Deventer, J. S. Afr. Inst. Min. Metall., 80 (1980) 239.
4 J.S.J. van Deventer, Thermochim. Acta, 112 (1987) 365.
5 T.J.W. de Bruijn, T.H. Soerawidjaja, W.A. de Jong and P.J. van den Berg, Chem. Eng. Sci., 35 (1980) 1591.
6 R.P. King and C.P. Brown, Metall. Trans. B, 11B (1980) 585.
7 O. Levenspiel, Chemical Reaction Engineering, Wiley, New York, 2nd edn., 1972, p. 368.